

Formation of Fluorescent Carbon from Fast Pyrolysis of Lignocellulosic Biomass

Carmela Russo, Francesca Cerciello, Osvalda Senneca, Anna Ciajolo, Barbara Apicella*

Istituto di Scienze e Tecnologie per l'Energia e la Mobilità Sostenibili, STEMS- CNR P.le Tecchio 80, 80125 Napoli, Italy*
barbara.apicella@stems.cnr.it

Fluorescent carbon was produced from fast pyrolysis of lignocellulosic biomass in a modified wire-mesh reactor named heated strip reactor (HSR). The metal grid, usually employed as a sample holder in a wire-mesh reactor, is replaced in the HSR by a pyrolytic graphite foil. HSR can achieve temperatures up to 2073 K with a high heating rate (104 K/s). The volatiles produced by the HSR pyrolysis of a lignocellulosic biomass sample were immediately quenched in the surrounding low temperature environment, so avoiding the occurrence of secondary reactions of the volatiles. Volatiles were condensed in form of a tar-like material on a pyrex glass bridge located above HSR, whereas the residue solid (char and soot) remained on the strip. The tar-like material recovered and separated with different solvents in fractions of various characteristics showed blue and/or green fluorescence typical of fluorescent carbon dots (CDs). It was thus shown that fast pyrolysis of carbon resources as biomasses, can be employed as one-step approach to synthesize different classes of carbon materials, assimilable to CDs. The different CDs could be separated and isolated choosing appropriate organic solvents and constitute very promising materials for applications in photonics, electro-optics, chemical sensing, and other material science areas.

1. Introduction

Carbon dots (CDs) are a new type of carbon-based zero-dimensional material and have drawn significant attention since the discovery of carbon fluorescent nanoparticles into arc discharge soot in 2004 [Xu et al. 2004]. CDs are eco-friendly candidates aiming at replacing both the semiconductor quantum nanodots and the organic dyes for biolabeling and bioimaging, as they offer great advantages due to their low toxicity and high biocompatibility, chemical stability and quantum yield. The synthesis of CDs from renewable biomass is especially attractive due to its sustainable and cost-efficient feature, therefore there is a growing research work on this topic, collected in some recent reviews [Kang et al 2020; Meng et al 2019; Zhao et al. 2020; Li et al. 2021].

Due to its versatility and simple experimental setup, hydrothermal carbonization has now become the most common procedure adopted for the production of CDs from natural biomass or other readily available carbon sources [Meng et al 2019]. However, hydrothermal methods are generally considered time-consuming and present disadvantages regarding the use of commodity chemicals [Heidari et al 2019; Kang et al 2020].

The present paper shows for the first time that fluorescent carbon featuring CD properties can be produced from fast pyrolysis (reaction times of order of seconds) of a lignocellulosic biomass in a modified wire-mesh reactor named heated strip reactor (HSR). Specifically, in this work fluorescent carbons produced in N₂ and CO₂ atmosphere from the pyrolysis of hemicellulose, one of the major components of lignocellulosic biomass, were analysed.

2. Experimental

Figure 1 shows a picture of the experimental apparatus used for treating the hemicellulose sample at severe heating conditions in N₂ or CO₂ atmosphere using a special heated strip reactor (HSR), where the metal grid, usually employed as a sample holder, is replaced by a pyrolytic graphite foil thermally stabilized for use up to

2800 K. Hemicellulose sample was supplied by Carl Roth GmbH+Co and consisted in a sample of Xylooligosaccharide (from Corncob) of granulometry smaller than 100 μm [Senneca et al. 2020]. For the experimental campaign a heating rate of 10^4 K/s was used [Senneca et al. 2010].

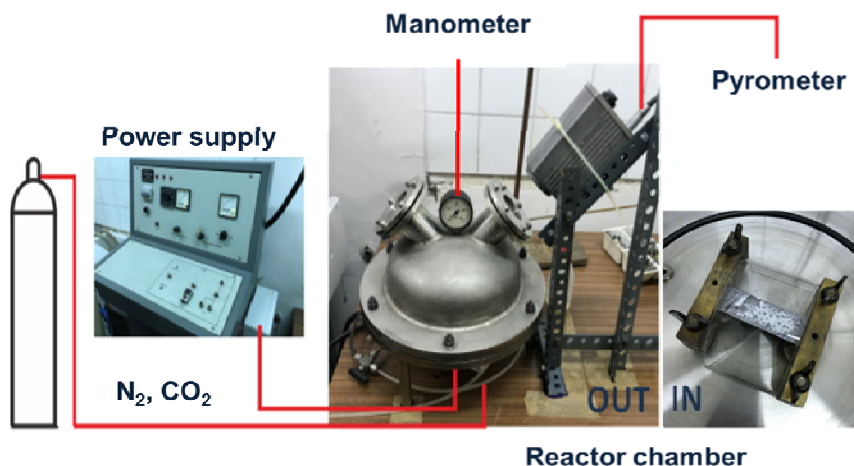


Figure 1. The heated strip reactor.

The apparatus is enclosed in a stainless-steel vessel with a volume of 2 L. The temperature of the grid is set by changing the value of the voltage at the two ends of the strip and is measured using a Pyrometer (Land System 4). For each test about 100 mg of fine particles were placed on the strip in a thin layer. The reactor was flushed with the test gas (N₂ or CO₂) for 10 min to remove any air traces. The strip was then heated up to the temperature of 2073 K and held at this temperature for 3 s. The pressure of the vessel was set at 2 bar. In a previous paper [Senneca et al 2010], modelling results, validated by thermocamera measurements, demonstrated that the particles temperature closely follows that of the graphite strip and that internal temperature gradients are limited to 50 K due to the small particles size.

A pyrex glass bridge located above the strip was cool enough to allow the condensation of the emitted volatiles in form of tar-like species. The species condensed on the Pyrex bridge were recovered by washing the support with acetone in ultrasonic bath. The acetone soluble fraction was named "acetone-tar". The solution volume was reduced to 0.5 ml under vacuum for analysis by gas chromatography- mass spectrometry (GC-MS). The GC-MS employed is an AGILENT GC 6890 - MSD 5975C. The mass spectrometer operating in electron ionization mode scanned m/z values in the range 50-400 u. In some conditions, acetone was unable to dissolve all the material deposited on the support. In these cases, the residue was dissolved in N-methyl pyrrolidone (NMP) and named "NMP-tar" [Apicella et al 2020].

Size Exclusion Chromatography (SEC) of NMP-tar samples was carried out on a HPLC system HP1050 series by elution with NMP on a Jordi Gel DVB Solid Bead column 300x7.8 mm for the molecular weight (MW) determination in the 2,000- 400,000,000 u range [Apicella 2003]. A HP1050 UV-Visible diode array detector was used for online detection of species eluted from the SEC column at a fixed absorption wavelength of 350 nm. UV-Visible spectra of the samples, dissolved in acetone or NMP, were measured on an HP 8453 Diode Array spectrophotometer using 1 cm quartz cuvettes [Alfè et al.2007]. Fluorescence spectra were acquired by a PerkinElmer LS-50 spectrofluorimeter using a xenon discharge lamp as excitation light source and a gated photomultiplier as detection device with modified S5 response for operation to about 650 nm. Monk-Gillieson type monochromators covered the following ranges: excitation of 200–800 nm and emission of 200–900 nm. The wavelength accuracy was ± 1.0 nm, and the wavelength reproducibility was ± 0.5 nm. Instrumental parameters were controlled by the Fluorescence Data Manager PerkinElmer software. Fluorescence measurements were performed on very diluted solutions samples to avoid concentration quenching and/or other phenomena that could distort the spectral shape affecting the fluorescence intensity. Synchronous fluorescence spectra were measured by applying a simultaneous scanning of the excitation and emission wavelengths, keeping constant the difference between the wavelengths ($\Delta\lambda = 10$ nm) [Apicella et al 2004].

3. Results

Figure 2, reports the photos of the tar sample solutions under UV light (365 nm) to show how acetone- and NMP-tar produced in N₂ environment from xylan at 2073K are able to exhibit fluorescence emission in the blue and in the green wavelength range, respectively.

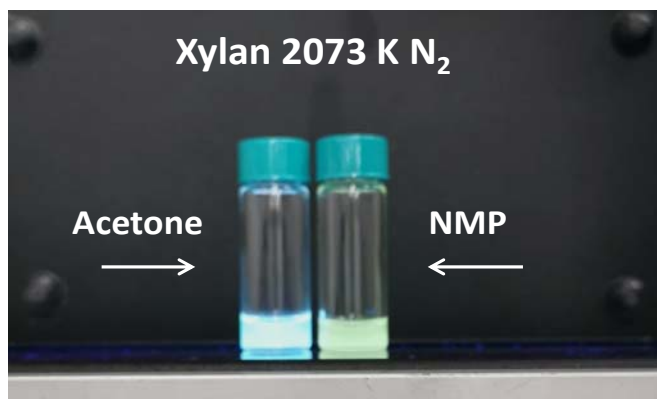


Figure 2. Photo under blue light irradiation of the tar sample dissolved in acetone and NMP collected after treatment of xylan in N₂

Consistently with the visible emissions in blue and green regions (Figure 2) the fluorescence spectra excited at different wavelengths reported in Figure 3 show the emission of acetone-tar more shifted toward the blue (350-600 nm) in comparison to the NMP-tar (400-700nm).

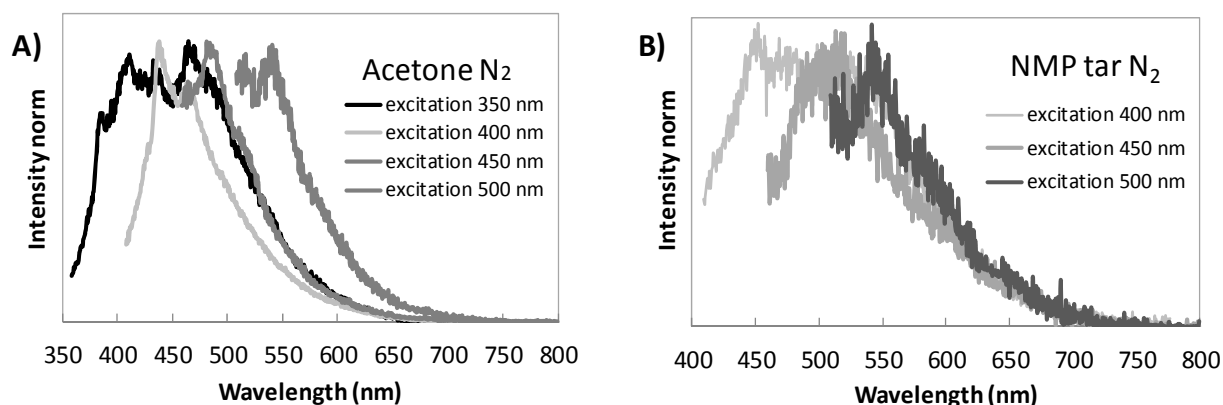


Figure 3 Normalized fluorescence spectra of acetone-tar (left) and NMP-tar CDs (right) excited at different wavelengths.

Overall, the acetone-tar fraction has shown to have a relatively simple composition [Senneca et al 2020]. As matter of fact, the main component detectable by GC-MS (>80%) of the acetone-tar obtained from hemicellulose resulted to be rare sugars as Levoglucosane and D-Allose. Phenols (alkyl-substituted) (about 13%) and light polycyclic aromatic hydrocarbons (PAH) up to 4 rings (fluoranthene and pyrene, 5%) could be also identified.

It is worth to note that no acetone-tar was produced in CO₂ environment. Moreover, it has to be mentioned that the NMP-tar fraction could be analyzed by SEC due to the low volatility of the NMP solvent hindering GC-MS analysis.

The UV-Visible and the synchronous fluorescence spectra of the acetone-tar fraction in N₂ are reported in Figure 4.

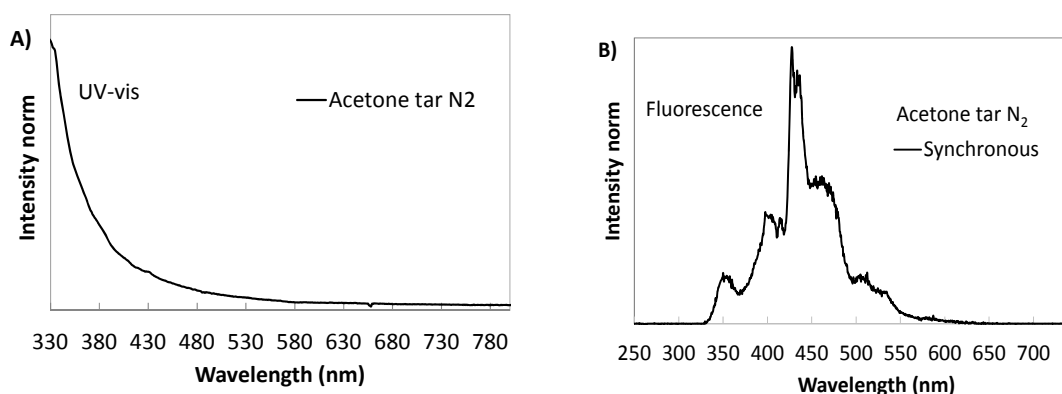


Figure 4. Spectra of acetone-tar fraction in N_2 : A) UV-Visible spectrum; B) synchronous fluorescence spectrum.

The acetone-tar presents the absorption steeply decreasing from UV toward the visible, ascribable to the presence of phenols and small PAH, typically absorbing in this range. Due to acetone interference in the UV (up to 310nm) the rare sugars absorption could not be observed as it is located in the range 200-290 nm (with maximum around 270 nm) [Kajjanen et al 2015]. The synchronous fluorescence spectrum, involving the simultaneous scanning of excitation and emission wavelengths using a $\Delta\lambda = 10$ nm exhibits peaks indicating significant presence of individual fluorescent molecules as PAH from 2 up to 5 rings [Russo et al 2019, Russo et al 2020], consistently with the GC-MS analysis and the fluorescence emission spectrum at different wavelengths reported in Figure 3. This emission shifts to a higher wavelength region at higher wavelength emission. The large presence of rare sugars, which do not contribute to fluorescence of the tar fraction, could be useful for make this fraction soluble in water, increasing the advantage of its potential application as CD. This important aspect will be deepened in a future work.

The SEC chromatograms of the NMP-tar fraction in N_2 and CO_2 [Senneca et al 2020] are reported in Figure 5. The SEC profiles are representative of the molecular weight (MW) distribution of the species present in the tar, since the retention time is inversely related to the molecular weight: the lower the retention time, the higher the mass of the eluting species. The curves present two or three peaks, depending on the sample. The first peak, observed only for the sample produced in N_2 , corresponds to the heaviest compounds of very high MW, around $3.7 \cdot 10^8$ u.

Assuming a density of 1.5 g/cm^3 and spherical size, this MW corresponds to molecule aggregates of size of 100 nm. The other two peaks at about 7.5 and 6.8 min correspond to MW of $3 \cdot 10^4$ u and 10^6 u, corresponding to sizes of 4 nm and 15 nm, respectively. The comparison of the SEC profiles clearly shows that CO_2 environment reduces the formation of very large size species (of about 100 nm).

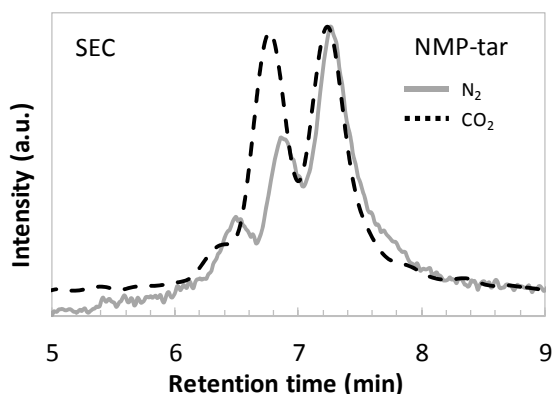


Figure 5. SEC analysis of the NMP-tar fraction collected in N_2 and in CO_2 ;

Figure 6A reports the UV-Visible spectra of NMP-tars, which exhibit a broader absorption with a tail extended into the visible wavelength range. This spectral feature underlines the more complex structure of the species composing NMP-tar, characterized by large aromatic structure strongly absorbing at high wavelengths. The N_2 sample presents a higher absorption in the visible due to the larger extension of aromatic moieties, featuring higher mass as it can be observed in the SEC chromatogram (Figure 5).

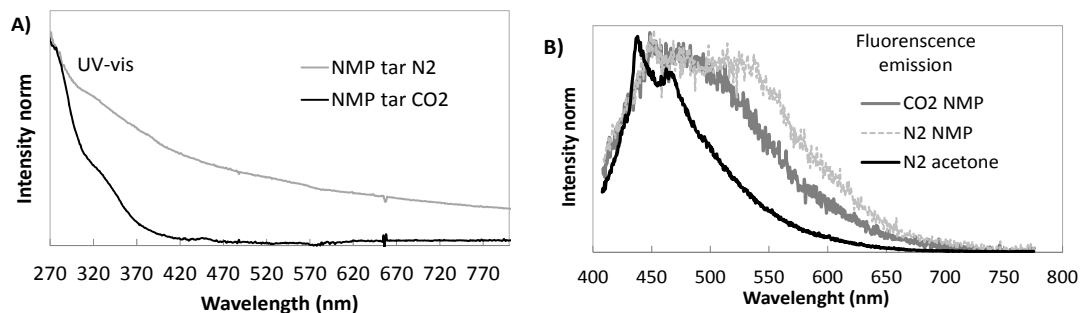


Figure 6. A) UV-Visible spectra of the NMP tar fraction in N_2 and CO_2 ; B) Normalized Fluorescence spectra excited at 400 nm of NMP-tar (N_2 and CO_2) and N_2 acetone-tar.

The emission spectra of NMP- and acetone-tar measured at an excitation wavelength of 400 nm are displayed in Figure 6B. In the case of NMP-tar the emission spectra are broader and there is a downward shift of the fluorescence signal toward the green region (500-570 nm), due to the presence of larger fluorescent species. Slight differences can be observed between the two NMP-tar emission (Figure 6B), underlying that even if the absorbing species are different (Figure 6A), fluorophores are similar.

Unlike the acetone-tar fraction, the nearly excitation-independent spectra of the NMP-tar (right panel of Figure 3) are indicative of homogenous macromolecular nature indicated by the broad UV-Visible spectrum (Figure 6A) and also consistent with the size of NMP-tar fraction, mainly in the range 4-15 nm.

4. Conclusions

In the present work it has been shown for the first time that HSR is a suitable reactor for the synthesis of easily separable blue and green fluorescent classes, assimilable to CDs, from non-toxic carbon resources (biomasses).

The best condition is the use of N_2 atmospheres, obtaining the blue carbon fraction with a large contribution of rare sugars (>80%), which do not contribute to fluorescence, but increase water solubility, and the green carbon fraction with dimensions of 4-15 nm.

Further work will be necessary for improving the optimization of operative conditions and the understanding of the properties of these fractions as the synthetic method appears to be very promising in terms of operation time of both reaction and fraction separation.

References

- Alfè, M.; Apicella, B.; Barbella, R.; Tregrossi, A.; Ciajolo, A. 2007, Similarities and dissimilarities in n-hexane and benzene sooting premixed flames, *Proc. Combust. Inst.*, 31 (1): 585-591.
- Apicella B., Barbella R., Ciajolo A., Tregrossi A., 2003, Comparative analysis of the structure of carbon materials relevant in combustion, *Chemosphere*, 51, 1063-1069.
- Apicella, B., Tregrossi, A., Ciajolo, A., 2004, Fluorescence Spectroscopy of Complex Aromatic Mixtures, *Anal. Chem.* 76, 2138-2143.
- Apicella B., Russo C., Cerciello F., Stanzione F., Ciajolo A., Scherer V., Senneca O., 2020, Insights on the role of primary and secondary tar reactions in soot inception during fast pyrolysis of coal, *Fuel*, 275, 117957.
- Heidari M., Dutta A., Acharya B., Mahmud S., 2019, A review of the current knowledge and challenges of hydrothermal carbonization for biomass conversion, *J. Energy Inst.*, 92(6), 1779-1799.
- Kajjainen L., Paakkunainen M., Pietarinen S., Jernström E., Reinikainen SP., 2015, Ultraviolet detection of monosaccharides: Multiple wavelength strategy to evaluate results after capillary zone electrophoretic separation. *International Journal of Electrochemical Science*, 10(4), 2950–2961.
- Kang C., Huang Y., Yang H., Fang Yan X., Ping Chen Z., 2020, A Review of Carbon Dots Produced from Biomass Wastes, *Nanomaterials*, 10, 2316.

- Lin X., Xiong M., Zhang J., He C., Ma X., Zhang H., Kuang Y., Yang M., Huang Q., 2021, Carbon dots based on natural resources: Synthesis and applications in sensors, *Microchemical Journal*, 160, 105604.
- Meng W., Bai X., Wang B., Liu Z., Lu S., Yang B., 2019, Biomass-Derived Carbon Dots and Their Applications, *Energy Environ. Mater.*, 2, 172–192.
- Russo C, Apicella B., Tregrossi A., Oliano M.M., Ciajolo A., 2020, Thermophoretic sampling of large PAH ($C \geq 22-24$) formed in flames, *Fuel*, 263, 116722.
- Russo C., Apicella B., Ciajolo A., 2019, Blue and green luminescent carbon nanodots from controllable fuel-rich flame reactors. *Sci Rep*, 9, 14566.
- Senneca O., Allouis C., Chirone R., Russo, S., 2010, Set up of an experimental apparatus for the study of fragmentation of solid fuels upon severe heating, *Exp. Therm. Fluid. Sci.*, 34, 366-372.
- Senneca O., Cerciello F., Russo C., Wutscher A., Muhler M., Apicella B., 2020, Thermal treatment of lignin, cellulose and hemicellulose in nitrogen and carbon dioxide, *Fuel*, 271, 117656.
- Xu X., Ray R., Gu Y., Ploehn H.J., Gearheart L., Raker K., Scrivens WA., 2004, Electrophoretic analysis and purification of fluorescent single-walled carbon nanotube fragments, *J. Am. Chem. Soc.*, 126, 12736–12737.
- Zhao, Y., Jing S., Peng X., Chen Z., Hu Y., Zhuo H., Sun R., Zhong L., 2020, Synthesizing green carbon dots with exceptionally high yield from biomass hydrothermal carbon. *Cellulose* 27, 415–428.